Study of the synchrotron and inverse Compton radiations of relativistic jets in GRS 1915+105

A.M.Atoyan[1,2] and F.A.Aharonian[1]

(1) Max-Planck-Institut für Kernphysik, Heidelberg, Germany
(2) Yerevan Physics Institute, Yerevan, Armenia

Abstract

We show that comparison of the detailed calculations of the synchrotron radiation of expanding magnetized clouds (plasmoids) with the temporal and spectral evolution of radio flares observed from the recently discovered galactic "microquasar" GRS 1915+105 imposes strong constraints on the model parameters of relativistic plasmoids, in particular, on the absolute values and time-dependence of the magnetic field, speed of expansion of radio clouds, the rates of injection of relativistic electrons into and their energy-dependent escape from the clouds, etc. The data of radio monitoring of the pair of ejecta not only enable unambiguous determination of the aspect angle and the speeds of propagation of both components, but also contain an important information about the energy source for acceleration of the electrons, in particular, may distinguish between the scenarios of bow-shock powered and magnetized relativistic wind powered plasmoids. Within the framework of the synchrotron-self-Compton model we also calculate the fluxes of synchrotron hard X-rays and GeV/TeV inverse Compton γ-rays, and discuss constraints on the parameters of GRS 1915+105 which could be provided by positive detection or flux upper limits of these energetic photons.

1 Introduction

The galactic black hole (BH) candidate source GRS 1915+105, discovered in 1992 as a hard X-ray transient (Castro-Tirado et al. 1994), attracts an extreme interest since the detection of superluminal radiojets in this source by Mirabel & Rodriguez (1994; hereafter MR94). Together with the second galactic superluminal jet source GRO J1655-40 (Tingay et al. 1995; Hjellming & Rupen, 1995), they constitute a new class of objects called *microquasars* (MR94), representing a scaled down analogs of QSOs (or generally AGNs) in two principal aspects: both microquasars and quasars are most probably powered by accretion onto BHs, although of essentially different mass scales, and both populations produce relativistic jets. Being, however, much closer to us than AGNs, the microquasars enable radio monitoring of not only approaching but also receding ejecta (importantly, in short timescales), which makes them unique cosmic laboratories for study of the phenomenon of relativistic jets (MR94).

Here we summarize the basic results of our recent study (Atoyan & Aharonian, 1997; AA97) of the prominent March/April 1994 radio flare of GRS 1915+105, when the approaching (*south*) and receding (*north*) ejecta moving in opposite directions with a speed $\beta \simeq 0.92$ at an aspect angle $\theta \simeq 70^\circ$ have been resolved, and superluminal speed $1.25\,c$ (for $d = 12.5\,$kpc) has been discovered (MR94).

2 General scenario

Comprehensive discussion of radio flares observed from GRS 1915+105, which most probably are connected with ejection of radio emitting material (i.e. clouds, containing relativistic electrons and magnetic fields frozen in the co-moving plasma), is given in MR94, Rodriguez et al. (1995), Foster et al. (1996). Here we would emphasize two important features of time evolution of the flares:
(**a**) a rapid, less than a day, rise time of the fluxes, $S_\nu \propto \nu^{-\alpha_{\rm r}}$, revealing transition from optically thick ($\alpha_{\rm r} \leq 0$) to thin ($\alpha_{\rm r} > 0$) emission, which is a typical signature of an expanding radio source;
(**b**) the spectral index $\alpha_{\rm r} \sim 0.5$ at the stages of flare maximum later on steepens to $\alpha_{\rm r} \sim 1$.

The study of these features results in conclusive information on the intrinsic parameters of the radio source. Indeed, modeling the ejecta (in its rest frame) as a spherical source of a radius R and magnetic field B, with a power-law distribution of relativistic electrons $N(\gamma) \propto \gamma^{-2}$ extending to $\gamma \geq 10^4$, we can express R and B in terms of $S_* \equiv S_{10\,\mathrm{GHz}}/500\,\mathrm{mJy}$ and cloud's opacity $\tau_\nu = R \times \kappa_\nu$ (κ_ν is the synchrotron absorption coefficient) at a frequency ν as (AA97):

$$B \simeq 0.15\,\delta^{7/17}\eta^{-4/17}S_*^{-2/17}\tau_\nu^{6/17}\nu_{\mathrm{GHz}}^{18/17}\ \mathrm{G}\,, \tag{1}$$

$$R = \ 4.6\times10^{14}\,\delta^{-28/17}\eta^{-1/17}S_*^{8/17}\tau_\nu^{-7/17}\nu_{\mathrm{GHz}}^{-21/17}\,\mathrm{cm}\,, \tag{2}$$

where $\nu_{\mathrm{GHz}} \equiv \nu/1\,\mathrm{GHz}$, $\delta = \sqrt{1-\beta^2}/(1-\beta\cos\theta) \simeq 0.57$ is the Doppler factor, and $\eta = w_\mathrm{e}/w_\mathrm{B}$ is the ratio of the electron to magnetic field energy densities. For the outburst of 19 March 1994, the fluxes measured at instant $t_0 \simeq 4.8$ days after ejection (the time of VLA observations on March 24.6), corresponded to $S_* \simeq 1$. Therefore, as it follows from Eq.(2), for optical transparency $\tau_\nu \leq 1$ apparent down to $\nu \simeq 1.4\,\mathrm{GHz}$, one needs $R \geq 8\times10^{14}\,\mathrm{cm}$. To reach that size during $t_0' = \delta\,t_0 \simeq 2.7$ days, the radio clouds should expand in their rest frame with a speed $v_\mathrm{exp} > 0.1\,c$. This agrees with the speed of expansion deduced directly from observations, and suggests that the lack of detection of red-shifted optical lines might be due to large Doppler-broadening of the lines (Mirabel et al. 1997).

For $\tau_{1.4\,\mathrm{GHz}} \leq 1$ Eq.(1) results in $B \leq 0.2\eta^{-4/17}\,\mathrm{G}$ at times $t \simeq t_0$. For the equipartition ($\eta = 1$) magnetic field $B_\mathrm{eq} \sim 0.2\,\mathrm{G}$ the synchrotron cooling time of electrons emitting at frequencies $\nu \sim 10\,\mathrm{GHz}$ exceeds few years. Therefore the synchrotron losses cannot be responsible for the observed steepening of radio spectra to $\alpha_\mathrm{r} \simeq 1$, which requires a steepening of the electron spectrum $N(\gamma,t)$ to an index $\alpha_\mathrm{e} \simeq 3$. We suggest a model (AA97) which attributes the steepening of $N(\gamma,t)$ to (i) *continuous injection* of relativistic electrons into the radio cloud, with the rate $Q(\gamma,t) \propto \gamma^{-2}q(t)$, *and* (ii) *energy-dependent escape* $\tau_\mathrm{esc}(\gamma,t) \propto \gamma^{-1}$ of the electrons from the cloud.

3 The March/April radio flare of GRS 1915+105

For calculations of the nonthermal radiation expected during radio flares, we have to find temporal evolution of the energy distribution of electrons $N(\gamma,t)$ in an expanding magnetized cloud. Generally, the equation for $N(\gamma,t)$, including the therm for stochastic *in-situ* acceleration, represents the partial differential equation of the second order (e.g. see Kardashev 1962). However, in the cases when the region of particle acceleration can be distinguished from the region of bulk emission, the acceleration terms can be effectively replaced by injection of accelerated particles into the radiation production region, which results in a well known differential equation of the first order:

$$\frac{\partial N}{\partial t} \ = \ \frac{\partial}{\partial\gamma}[P(\gamma,t)N] \ - \ \frac{N}{\tau_\mathrm{esc}(\gamma,t)} \ + \ Q(\gamma,t)\ . \tag{3}$$

For the parameters characterizing the radio clouds in GRS 1915+105, the energy losses $P = -(\mathrm{d}\gamma/\mathrm{d}t)$ of electrons in an expanding magnetized medium are mainly due to adiabatic losses, and at very high energies also the radiative losses. Assuming the temporal evolution of magnetic field in the form of $B(t) = B_0(R/R_0)^{-m}$, where $R = R(t)$ and $R_0 \equiv R(t_0)$, we have $P = v_\mathrm{exp}\,\gamma/R + p_2\gamma^2/R^{2m}$ ($p_2 = \mathrm{const}$). Assuming $v_\mathrm{exp} = \mathrm{const}$, we have found (AA97) analytical solution to Eq.(3). This solution can be used in numerical calculations for an arbitrary time dependence of $v_\mathrm{exp}(t)$, if approximating the latter by the mean $\bar{v}_\mathrm{i}$ in small time intervals Δt_i.

Allowing for a (natural) deceleration of cloud's expansion at later stages, we suppose $v_\mathrm{exp} = v_0/(1+t'/t_\mathrm{exp})^k$, where t' is in the rest frame of the ejecta. The injection rate is taken as $Q(\gamma,t') \propto \gamma^{-\alpha_\mathrm{inj}}\exp(-\gamma/\gamma_\mathrm{c})\,q(t')$, which implies that the shape of energy spectrum (power law with exponential

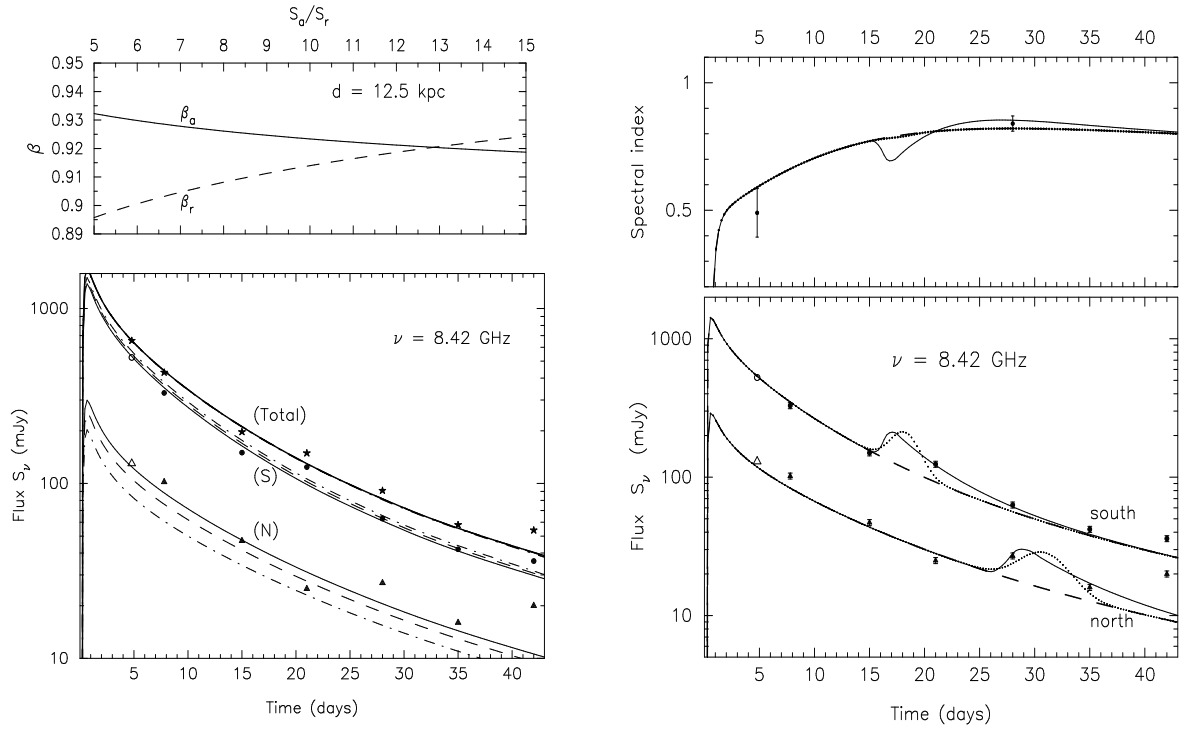

Fig.1 a (left): *Top panel* – The speeds of approaching (solid line) and receding (dashed line) ejecta calculated from Eq.(4) for different ratios of $S_{\rm a}/S_{\rm r}$. In the symmetric case, $\beta_{\rm a} = \beta_{\rm r}\,(= 0.920)$, the aspect angle is $\theta = 69.6°$, resulting in $S_{\rm a}/S_{\rm r} = 12.8$; *Bottom panel* –Evolution of the radio fluxes from the south (S) and north (N) radio components expected in the case of identical ejecta with $\beta_{\rm a} = \beta_{\rm r}$ (dot-dashed lines), and slightly asymmetrical ones, with $S_{\rm a}/S_{\rm b} = 7$ (solid lines) and 9 (dashed lines). Note that the total fluxes coincide.

Fig.1 b (right): The time evolution of the radio fluxes and spectral indexes at 8.42 GHz, expected in the case of synchronous increase (by factor of 2) of the injection rate of relativistic electrons into the south and north radio clouds during $\Delta t \leq 1$ day around *equal* intrinsic times $t' = 9$ days (solid curves). The dashed curves show the spectral evolution without an 'afterimpulse'. The dotted curves correspond to the case when the 'afterimpulse' is in the form of an increase of magnetic field by 40 %, while the injection of electrons proceeds smoothly. To distinguish the flux curves, somewhat different shapes of the 'magnetic' and 'electronic' afterimpulses are supposed. The *principal* difference between these 2 cases is in different time evolution of $\alpha_{\rm r}$.

cutoff) does not change in time. The term $q(t') = (1 + t'/t_{\rm inj})^{-p}$ defines the time profile of the electron injection rate. For the escape time we suppose energy dependence in the form $\tau_{\rm esc}(\gamma, t') \propto R^{-u}\gamma^{-\Delta}$ and take into account that $\tau_{\rm esc} \geq R/c$.

Model parameters

Comparison of the numerical calculations of synchrotron radiation of radio clouds with the fluxes detected during March/April flare (MR94; Rodriguez et al. 1995) prove that initial speed of expansion $v_0 \sim (0.1 - 0.2)\,c$ is needed, depending on the magnetic field B_0 at instant $t_0 = 4.8$ days after ejection. For the equipartition magnetic field, $B_{\rm eq} \simeq 0.2$ G, a typical power of injection of relativistic electrons $L_{\rm e} \sim (0.5 - 1) \times 10^{38}$ erg/s is required. However, $L_{\rm e}$ should be much higher if $B_0 < B_{\rm eq}$, e.g., $L_{\rm e} \geq 10^{39}$ erg/s for $B_0 \simeq 0.05$ G.

The observed rate of decline of the flare requires a decrease of $B(R) \propto R^{-m}$ with $m \simeq 1$. The

power law index $\alpha_{\rm inj} \simeq 2$ follows from the observation of $\alpha_{\rm r} \simeq 0.5$ on March 24, when the escape losses have not yet significantly modified the electron spectrum $N(\gamma, t)$. The observed steepening of the radio spectrum at $\sim 10\,$GHz from $\alpha_{\rm r} \simeq 0.5$ to $\alpha_{\rm r} \simeq 0.84$ on April 16 requires, in our model, an escape of the electrons with $\Delta \simeq 1$, and allows for some variation of the parameter $u \sim 1.5$. Importantly, the steepening of radio spectra can be explained only if the cloud's expansion after $t_{\rm exp} \sim (1-3)\,$days gradually decelerates, with $k \sim (0.7-1)$, *and* if about the same time (namely, $t_{\rm inj} \sim (1-2)\,t_{\rm exp}$) the injection of new particles declines with $p \simeq 2k$. Otherwise the escape of radio electrons from rapidly expanding cloud would not be fast enough to steepen $N(\gamma, t)$ as needed. Remarkably, an injection rate of this kind can be easily provided, in particular, if one would assume that it is proportional to the solid angle of the cloud as observed from the central source: $q(t') \to q_{\rm b}(t') = [R(t')/v_0 t']^2$. We prefer to call $q_{\rm b}(t')$ as the 'beam injection' case, and further on use this type of injection in order to reduce the number of free model-parameters.

Brightness ratio as a measure of South/North asymmetry

To explain the observed (MR94) brightness ratio of the approaching to receding ejecta $S_{\rm a}/S_{\rm r} = 8 \pm 1$ (instead of $S_{\rm a}/S_{\rm r} \geq 12$ expected for *identical* plasmoids), we suppose that the twin ejecta are *similar* but not identical (for another possibility see Bodo & Ghisellini, 1996), allowing for some asymmetry between the pair of ejecta in the speeds of propagation ($\beta_{\rm a} \neq \beta_{\rm r}$), aspect angles ($\theta_{\rm r} \neq 180^\circ - \theta_{\rm a}$) or intrinsic luminosities ($S'_{\rm a} \neq S'_{\rm r}$). In particular, the degree of South/North asymmetry needed is smallest if mainly the speeds $\beta_{\rm a}$ and $\beta_{\rm r}$ would be different. In this case for the ratio $S_{\rm a}/S_{\rm r}$ at equal *intrinsic times* we have

$$\frac{S_{\rm a}}{S_{\rm b}} = \left(\frac{\delta_{\rm a}}{\delta_{\rm r}}\right)^{3+\alpha_{\rm r}} = \left(\frac{\Gamma_{\rm r}}{\Gamma_{\rm a}}\right)^{3+\alpha_{\rm r}} \left(\frac{1+\beta_{\rm r}\cos\theta}{1-\beta_{\rm a}\cos\theta}\right)^{3+\alpha_{\rm r}} \quad . \tag{4}$$

Due to strong dependence of Eq.(4) on the ratio of Lorentz-factors $\Gamma_{\rm r}/\Gamma_{\rm a}$, a deviation of the ratio $S_{\rm a}/S_{\rm r}$ from the one expected for *identical* ejecta can be explained by a small difference between $\beta_{\rm a}$ and $\beta_{\rm r}$ (see top panel in Fig.1a). For example, solution of Eq.(4) together with the equations describing the apparent angular separation of the ejecta, results in $\beta_{\rm a} = 0.928$, $\beta_{\rm r} = 0.905$, $\theta = 70.3^\circ$ for $S_{\rm a}/S_{\rm r} = 7$. In this case the fluxes of both components seem to agree with the ones measured by MR94 (see Fig.1a, bottom panel). Note that for the given parameters of GRS 1915+105, the ratio $S_{\rm a}/S_{\rm r} = 7$ at equal *intrinsic times* corresponds to $S_{\rm a}/S_{\rm r} \simeq 8$ measured at equal *angular separations*.

Synchronous afterimpulses far away from the central source ?

The reported accuracy of VLA flux measurements in MR94 is $\sim 5\,\%$. Meanwhile some of the data points in Fig.1a, in particular the fluxes on 21-st day (April 9) for the south, and 28-th day (April 16) for the north components, exceed the calculated fluxes by $\gg 5\,\%$, therefore they still need a better explanation. We would like to believe that this discrepancy could be connected with significant increase of the fluxes between April 4 and 5 ($t = 16 - 17\,$days) detected by the Nancay telescope. It is seen from Table 1 and Fig.1 in Rodriguez et al (1995), that during 24 hours between these 2 days the fluxes at both 1.41 GHz and 3.3 GHz have suddenly *increased* by $\simeq 30\,\%$. Although VLA was not observing GRS 1915+105 at that days, the 'echo' of that event could be present in the flux detected by VLA from the approaching component on April 9. Also, one should expect significant *delay* between the times of VLA observations of that event from the *south* and *north* radio clouds, if it was due to powerful two-sided afterimpulse from the central source which has reached the two clouds at equal intrinsic times $t'_{\rm a} = t'_{\rm r}$. In Fig.1b we show the fluxes calculated for practically the same model parameters as in Fig.1a (for $S_{\rm a}/S_{\rm r} = 7$), but assuming that there was an additional short ($\Delta t' \leq 1\,$day) impulse of injection of relativistic electrons into *both* clouds around intrinsic times

$t' = 9$ days after ejection event. Taking into account different Doppler factors of counter ejecta, this intrinsic time corresponds to *apparent* times $t_{\rm a} = 16.6$ days and $t_{\rm r} = 27.5$ days for the approaching and receding components, respectively. It is seen from Fig.1b that agreement with the measured fluxes now becomes better. Note that the last two data points (on April 30) cannot be explained by another afterimpulse, since they coincide in time. The excess fluxes on that day are most probably connected with the second ejection event occured, as noted in MR94, around April 23.

If such an interpretation of the data is not just an artefact, but corresponds to reality, implications for the physics of jets may be very important: it could mean that both clouds continue to be energized by the central source being even far away from it (presumably, through a relativistic wind in the jet region, and perhaps also the wind termination *reverse* shock on the *back* side of the clouds), or otherwise we have to rely upon a mere coincidence of equal intrinsic times (as well as amplitudes) of additional injection of relativistic particles from the bow shocks ahead of two counter ejecta.

4 Predictions for nonthermal high energy radiation

GRS 1915+105 is a very strong transient X-ray source, with peak luminosities exceeding 10^{39} erg/s. This radiation most probably originates in the thermal plasma near the central compact object. In addition, nonthermal X-rays of synchrotron origin could be produced in the relativistic ejecta, if the spectrum of accelerated electrons there would extend beyond TeV energies as it is the case in blazars (e.g. see Urry & Padovani 1995). Although from the point of view of required energetics in jets it is obvious that the X-radiation of the jet generally cannot be responsible for the bulk of observed X-ray fluxes, the synchrotron component, however, may become visible at high energies, say $E_{\rm X} \geq 100$ keV, where the thermal emission is typically suppressed.

In Fig.2 we present the time evolution of the synchrotron and IC radiation fluxes in the range from radio to very high energy γ-rays expected in the case of cloud's magnetic field $B_0 = 0.05$ G, calculated for the injection spectrum of electrons with exponential cutoff around $E_{\rm c} = 30$ TeV. It is seen that during the first several hours after ejection (or somewhat more, depending on the actual time needed for formation/acceleration of the expanding ejecta), when the cloud is still opaque for synchrotron emission at GHz frequencies, the synchrotron fluxes may dominate over the extrapolation of thermal component at energies ≥ 100 keV. This may result in significant flattening of overal spectrum at $E_{\rm X} \sim 100$ keV. Interestingly, hard tails of X-ray spectra perhaps are a common feature of the galactic BH source population, among which is GRS 1915+105 (Harmon et al. 1994). Although an existence of such feature in the spectrum of GRS 1915+105 could be seen only marginally (see e.g. Sazonov et al. 1994), in case of the second microquasar GRO J1655-40 the X-ray spectra clearly extend up to several hundred keV (see Harmon et al. 1995).

The second signature of acceleration of TeV electrons in GRS 1915+105 could be detection of IC γ-rays. The calculations in the framework of synchrotron-self-Compton models, based on the parameters defined from radio observations, show that during the strong flares we may expect detectable fluxes of γ-rays , first of all at TeV energies, provided that the magnetic field in the radio clouds does not exceed 0.1 G. In Fig.2 we show the fluxes of IC γ-rays calculated for parameters of the March/April 1994 flare at 3 different times after the outburst. We can see that the γ-ray fluxes above several hundred GeV during first few hours of the flare are on the level of 3×10^{-11} erg/cm^{2}s, which is about of the VHE γ-ray flux of the Crab Nebula. After few days the flux drops to the level of 0.1 Crab which is still detectable by current Imaging Cherenkov telescopes in Northern hemisphere (CAT, HEGRA, Whipple). Afterwards the source becomes invisible.

Assumption of lower magnetic field results in higher (approximately $\propto B^{-2}$) γ-ray fluxes. However, as far as a magnetic field significantly less than 0.05 G would imply injection luminosity of electrons

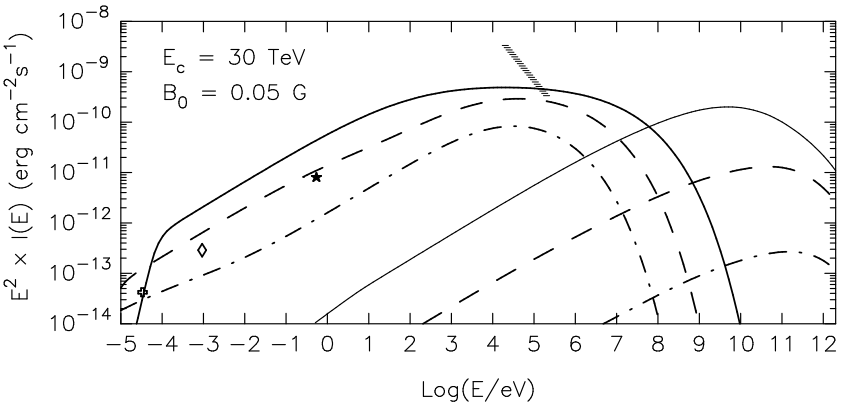

Fig.2: Broad band synchrotron (heavy lines) and IC (thin lines) radiation fluxes expected during a flare from GRS 1915+105 at $t = 0.1$ day (solid lines) $t = 1$ day (dashed lines) and $t = 10$ days (dot dashed lines) after relativistic ejection event. Data points correspond to the level of maximum radio fluxes observed at 8.4 GHz (the cross) and 234 GHz (diamond) (from Rodriguez et al. 1995). The star is for the flux of IR jet reported by Sams et al. (1996), and the hatched region shows the level of hard X-ray fluxes typically detected during the X-ray flares of GRS 1915+105 in the energy range ≥ 20 keV (Harmon et al. 1997). Magnetic field $B_0 = 0.05$ G is supposed, which implies $L_e = 3 \times 10^{39}$ erg/s.

$L_e \geq 10^{40}$ erg/s, it is difficult to expect γ-ray fluxes essentially exceeding the fluxes shown in Fig.2. On the other hand, in the case of magnetic field on the level of equipartition $B \simeq 0.2$ G or higher, the IC fluxes dramatically decrease. Therefore either positive detection or upper limits of VHE γ-ray fluxes, being combined with hard X-ray observations above 100 keV, could provide robust constraints on the magnetic field in the ejecta (or the luminosity L_e) and/or efficiency of acceleration of electrons beyond TeV energies.

Information about IC γ-rays can be obtained also in EGRET energy domain, i.e. at $E \geq 100$ MeV. However, it should be noted that even during the first few hours of the flare, the fluxes in this energy range do not exceed 10^{-6} ph/cm^{2}s. This implies that with the effective detection area of the EGRET $\sim 10^3$ cm^2, only several photons could be detected during the first day of the outburst. Unfortunately, since the IC fluxes significantly drop with expansion of the cloud, observations of the flare after that time could not noticeably improve the photon statistics.

References

Atoyan, A.M., and Aharonian, F.A. 1997, in preparation (AA97)
Bodo, G., and Ghisellini, G. 1995, ApJ **441**, L69
Castro-Tirado, A., et al. 1994, ApJS **92**, 469
Harmon, B.A., et al. 1994, The second Compton Symposium, AIP Conf. Proc. **304**, p.210
Harmon, B.A., et al. 1995, Nature **374**, 703
Harmon, B.A., et al. 1997, ApJ **477**, L85
Hjellming, R.M., and Rupen, M.P. 1995, Nature **375**, 464
Kardashev, N.S. 1962, Sov. Astron.-AJ **6**, 317
Mirabel, I.F., and Rodriguez, L.F. 1994, Nature **371**, 46 (MR94)
Mirabel, I.F., et al. 1997, ApJ **477**, L45
Rodriguez, L.F., et al. 1995, ApJS **101**, 173
Sams, B.J., Eckart, A., and Sunyaev, R. 1996, Nature **382**, 47
Sazonov, S.Y., et al. 1994, Astron. Lett. **20**, 787.
Tingay S.J., et al. 1995, Nature **374**, 141
Urry, M.C., and Padovani, P. 1995, PASP **107**, 803